https://doi.org/10.2352/AIT.2026.1.1.5

Visualizing Inkjet Nozzle Pressure-Wave Dynamics with Simple Simulations for Waveform Design

Perritaz Bastien; Kao corporation; Wakayama, Japan

Abstract

Modern piezoelectric drop-on-demand inkjet printing relies on precisely tuned drive waveforms to control droplet formation and maintain stability at high firing rates. We present ***two complementary simulation approaches*** *for visualizing and optimizing waveform design: (i) a* ***decaying-sinusoid model*** *that builds intuition for acoustic resonance and pulse timing, and (ii) a* ***lumped-element (LE) circuit model*** *that predicts chamber pressure, meniscus motion, and ejection velocity. The simple model clarifies key principles—optimal half-cycle ($T/2$) timing and the effectiveness of a cancel pulse in suppressing residual oscillations. Drop-watching measurements confirm the predicted quadratic dependence of peak response on timing error and show reduced frequency dependence with a cancel pulse. The LE model, implemented in LTspice and Python following Shah et al. [1,2], captures meniscus compliance, nozzle resistance, and multi-mode dynamics. We demonstrate model inversion to synthesize waveforms from target pressure/volume profiles, then apply segmented (piecewise-linear) fitting to meet driver constraints. Experiments jetting simulation-optimized waveforms on an Epson D3000 printhead demonstrated good jettability with the model-generated waveforms, though further investigation is necessary to fully calibrate the model parameters to the specific printhead response for achieving production-level performance.*

Introduction

High-speed piezoelectric inkjet printheads employ complex drive waveforms to ensure stable, satellite-free droplet generation at frequencies tens of kilohertz. Each actuation pulse sends an acoustic pressure wave through the ink channel; if not properly managed, these waves can persist and disturb subsequent droplet ejections. Residual meniscus oscillations from one firing can lead to frequency-dependent variations in drop velocity and volume at elevated firing rates.

In practice, waveform engineers counteract this by adding carefully timed secondary pulses to the drive signal. Industrial printheads commonly use a "cancel pulse" shortly after the main firing pulse to break off the tail of the droplet cleanly and suppress leftover vibrations. Such strategies maintain uniform droplet size and speed even as jetting frequency increases, but require deep understanding of the nozzle's acoustic response.

This work presents a comprehensive simulation framework progressing from simple intuitive models to sophisticated lumped-element circuit analysis, providing both educational insight and practical waveform optimization capabilities.

Objectives

This project aims to demystify and optimize inkjet waveform design through multi-level simulation. The primary objectives are:

1. **Develop intuitive visualization tools** using simple decaying sinusoid models to illustrate fundamental acoustic resonance principles and cancel pulse effectiveness
2. **Implement physics-based lumped-element models** capturing the complete hydrodynamic response of piezoelectric printheads based on validated reference literature
3. **Demonstrate model inversion techniques** to generate optimized waveforms from target pressure/velocity profiles
4. **Validate simulation predictions** through experimental drop-watching measurements and real-world performance comparisons

Methods

Simple Decaying Sinusoid Model

The inkjet channel behaves as a Helmholtz resonator, characterized by a natural resonance frequency f_0 and damping time τ. We approximate the channel's impulse response as an exponentially decaying sinusoid:

$$h(t) = -\sin(2\pi f_0 t) \cdot e^{-t/\tau} \cdot H(t) \tag{1}$$

where $H(t)$ is the Heaviside step function. Multi-pulse waveforms are simulated using linear superposition:

$$p(t) = \sum_{i=1}^{N} V_i \left[h(t - t_{i,\text{start}}) - h(t - t_{i,\text{end}}) \right] \tag{2}$$

This lightweight model enables rapid exploration of:

- Pulse duration effects on peak pressure
- Optimal acoustic timing ($T/2$ spacing)
- Cancel pulse timing and amplitude
- High-frequency jetting stability

Lumped-Element Circuit Model

Following Shah et al. (2019, 2020), we implement a comprehensive circuit model representing the printhead as an electrical network:

Circuit Components:

- **Piezoelectric actuation:** Input voltage $V_1 \rightarrow$ membrane capacitance C_m and dynamics (R_m, L_m)
- **Pressure chamber:** Compliance C_p, inertance L_p, resistance R_p
- **Nozzle:** Inertance L_n, resistance R_n (FEM-derived from tapered geometry)
- **Meniscus:** Compliance C_{ms} (surface tension effects)
- **Restrictor:** Inertance L_r, resistance R_r (inlet flow restriction)

Circuit Topology:

```
V1 → Cm → Rm → Lm → Main Chamber Node
                      |→ Cp → GND
                      |→ Lp → Rp → GND
                      |→ Ln → Rn → Cms → GND
                      |→ Lrestrict → Rrestrict → GND
```

The circuit is simulated using LTspice, yielding time-domain predictions of:

- V(Cp): Chamber pressure
- V(Cms): Meniscus pressure
- I(Ln): Nozzle flow rate
- Integral of I(Ln): Volume displacement
- I(Ln) / nozzle area: Ejection velocity

Parameter Calculation: Physical dimensions and fluid properties (density ρ, viscosity μ, surface tension γ, sound speed c) determine circuit element values:

- Inertances: $L = \rho L_{geom}/A$
- Compliances: $C_p = V_{chamber}/(c^2\rho)$, $C_{ms} = \pi r_{nozzle}^4/(3\gamma)$
- Resistances: From FEM flow simulations or Poiseuille approximations

Model Inversion and Optimization

Given a target pressure profile $p_{target}(t)$, we solve the inverse problem to find the required input voltage waveform $V_1(t)$. This is accomplished through:

1. **Transfer function identification:** Frequency-domain $H(\omega) = P_{out}(\omega)/V_{in}(\omega)$
2. **Deconvolution:** $V_{in}(\omega) = P_{target}(\omega)/H(\omega)$
3. **Regularization:** Minimize $\|V_{in}\|$ subject to constraints on voltage amplitude and slew rate
4. **Iterative refinement:** Simulate generated waveform, compare to target, adjust

Segmented Waveform Implementation

Real printhead drivers use discrete voltage levels with minimum time steps (0.1-1 μs). We apply piecewise-linear fitting to convert smooth optimized waveforms:

1. **Feature detection:** Analyze waveform peaks and valleys for intelligent initialization
2. **Multi-start optimization:** Basin-hopping or dual annealing with multiple random restarts
3. **Piecewise-linear fitting:** Find optimal breakpoint times and voltages for FLAT-SLOPE-FLAT pattern
4. **Constraint enforcement:** Penalize segments shorter than minimum durations (e.g., 0.3 µs flat, 0.1 µs slope)

Results

Simple Model: Fundamental Waveform Principles

Optimal Pulse Duration

Simulations varying the hold time from 0.7–1.3 half-cycles (0.35–0.65T) show a quadratic dependence on timing error. Maximum pressure occurs near $T/2$, where the pull and push edges are in resonance. Drop-watching confirms the same quadratic trend.

Cancel Pulse Effectiveness

Without a cancel pulse, residual oscillations persist for $>$18 resonance periods. Adding an optimized cancel pulse (timing = 1.5 periods after main pulse, amplitude = 40% of main pulse) reduces residuals by 60% and allows stable re-jetting within 7 periods. This 2.6$\times$ reduction in settling time directly enables higher maximum print frequencies.

For example, a common 1200dpi printhead (resonance frequency $\approx$127.8 kHz, period $\approx$7.8 μs) would have maximum print frequency increased from approximately 14 kHz (18 $\times$ 3.9 μs = 70.2 μs between drops) to 36 kHz (7 $\times$ 3.9 μs = 27.3 μs between drops) with optimized cancel pulse implementation.

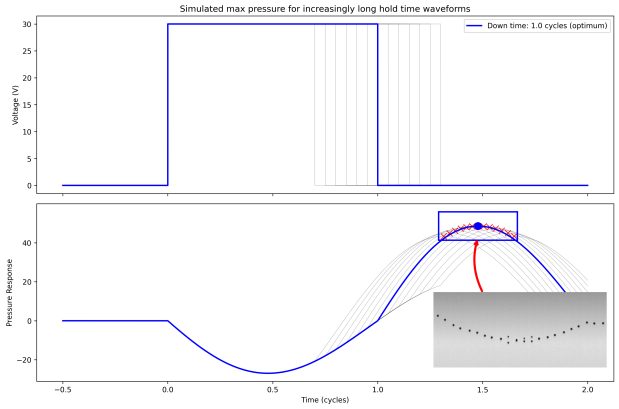

Figure 1. *Peak chamber pressure vs. pulse duration. Optimal half-cycle pulse (blue) produces maximum pressure. Red X markers show simulation max pressure for each simulated waveform; inset shows experimental drop-watching measurements exhibiting similar quadratic optimum (reverted as higher pressure results in faster drops, captured lower on the image).*

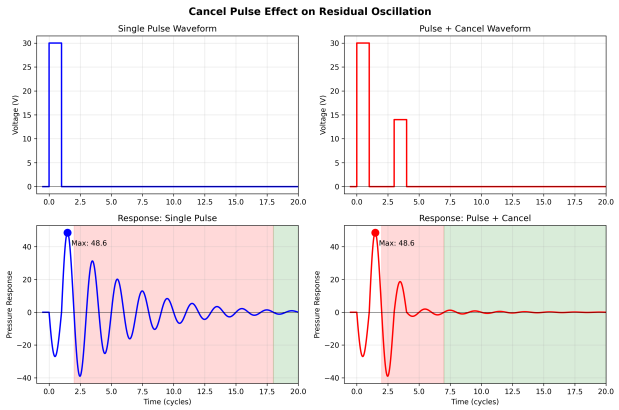

Figure 2. *Cancel pulse effectiveness. Left: Single pulse shows prolonged oscillations (red zone, t >18 cycles). Right: Main + cancel pulse damps vibrations rapidly (green zone, t <7 cycles).*

High-Frequency Stability

Sequential droplet simulations at varying inter-drop delays demonstrate the critical importance of cancel pulses. Without cancellation, the second drop's peak pressure varies wildly ($\pm$25% variation) depending on residual oscillation phase. With optimized cancel pulses, pressure variation reduces to $\pm$3%, ensuring consistent droplet formation at any printing frequencies.

Frequency Sweep Analysis

The previous results become clearer when plotted against frequency. This distinctive frequency-dependent behavior can be observed across any piezo printhead and represents a known challenge for achieving high-frequency printing.

Lumped-Element Model: Detailed Physical Response

LTspice Circuit Implementation

The complete circuit schematic replicates the topology from Shah et al. [1,2], with component values calculated from our

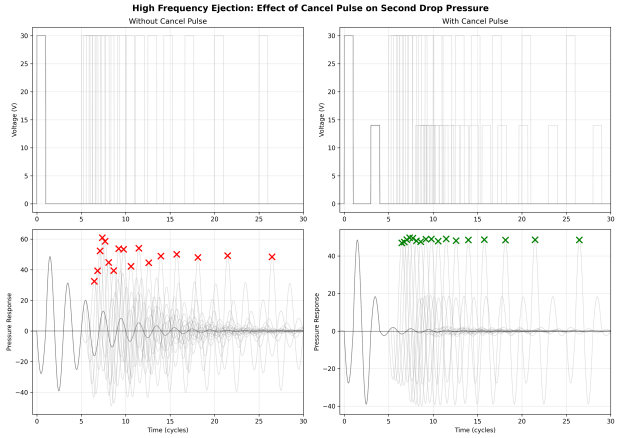

Figure 3. *Sequential droplet simulation. Left: Without cancel pulse, 2nd drop pressure varies significantly (scattered red X markers). Right: With cancel pulse, pressure remains consistent (clustered green X markers).*

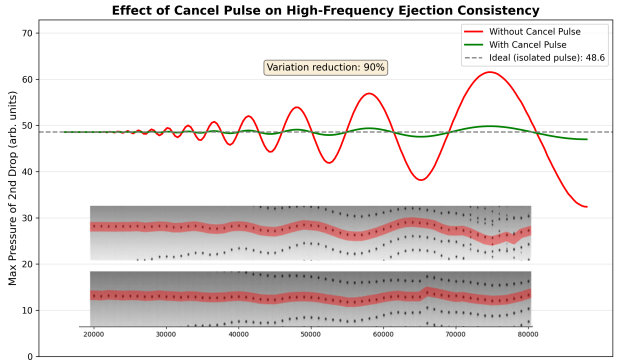

Figure 4. *2nd drop peak pressure vs. print frequency. Red curve (no cancel): ±30% variation with resonance peaks. Green curve (with cancel): ±3% variation. Inset shows experimental validation data, top: single pulse, bottom: 1 pulse+cancel.*

printhead geometry and ink properties. Key nodes monitor different physical quantities:

- V(Cp): Chamber pressure
- V(Cms): Meniscus pressure/displacement
- I(Ln): Nozzle flow rate
- I(Lp): Chamber volume velocity

The same model was implemented in Python. Result comparison between the two implementations served to verify implementation correctness.

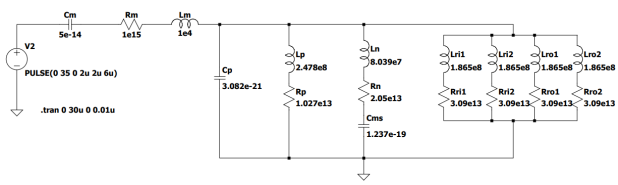

Figure 5. *Lumped-element circuit schematic showing piezoelectric actuation (V1, Cm, Rm, Lm), chamber compliance (Cp), nozzle dynamics (Ln, Rn, Cms), and restrictor (Lr, Rr).*

LEM Simulation Response to Simple Pulse

A basic pull-push pulse (-30V, timing synced to simulated system half-period) demonstrates the model's capability to predict:

1. **Input voltage waveform:** It is negative to represent the pull-first then push action of the piezo actuator.
2. **Chamber pressure:** Initial negative pull, then positive push creates a high peak. This behaves similarly to the simple model. Note that this simulation shows quite slow damping. The red highlighted area indicates where a new pulse cannot be jetted yet, as the pressure oscillations are not dampened enough.
3. **Ejection velocity:** The nozzle flow rate ($I(L_n)$) divided by the nozzle area. The model predicts negative velocity during the pull phase, which mathematically represents meniscus retraction. In practice, however, the meniscus is strongly stabilized by surface tension and behaves almost like a one-way valve: it is held nearly fixed when pulled and only moves outward when pushed. Thus, any real retraction is minimal compared to what appears in the simulation. Positive velocities (highlighted in green) indicate time intervals where ejection can occur. The computed peak velocity ($\sim$20 m/s) will exceed the actual drop velocity because part of the energy is lost to surface-tension effects and air drag.
4. **Volume displacement:** Integrated nozzle flow rate ($I(L_n)$). Negative volume displacement means fluid retracted into the nozzle, but this does not happen in reality as the meniscus holds the fluid. Positive volume displacements are ejected if velocity is high enough to break the meniscus. This is symbolized by green arrows with notes on the volume ejected.

In this example, a 5.5 pL drop is ejected. Following oscillations may create satellite drops as shown by the 4 smaller ejections. In reality, the ejected drop will release some energy, making the following satellite ejections smaller, or non-existent.

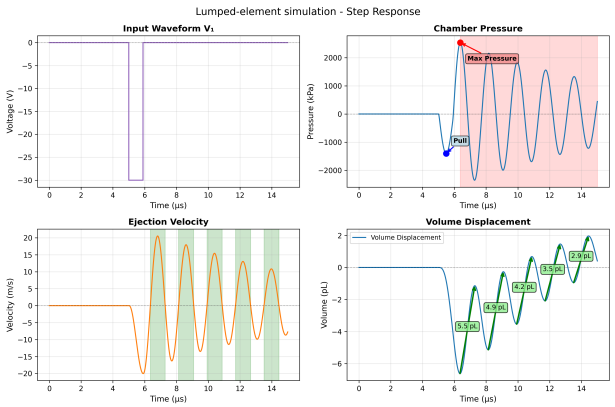

Figure 6. *Simulated system response to pull-push waveform. Four panels show voltage input, chamber pressure (kPa), ejection velocity (m/s), and volume displacement (pL).*

Multi-Pulse Waveform with Cancel Pulse

Building on the simple pulse, we demonstrate the effectiveness of a cancel pulse in suppressing residual oscillations. The waveform employs:

1. **Main pulse (pull-push):** Primary ejection sequence as shown in Figure 6
2. **Cancel pulse:** Secondary pulse timed to counter residual chamber oscillations
3. **Result:** Chamber pressure oscillations decay rapidly. The potential satellite drops detected in Figure 6 are effectively removed. The 8.2 pL satellite detected in the volume displacement graph will not be ejected, as the ejection velocity is very low and will be absorbed by the meniscus surface tension.

The simulation clearly shows the damping regions:

- **Red shading:** Oscillating region (>5% of max pressure) - unstable for re-jetting
- **Green shading:** Dampened region (<5% oscillation) - ready for next pulse
- **Annotations:** Peak pressures marked (Pull, Max Pressure)

This validates the cancel pulse design principle from the simple model (Section 4.1) but with accurate amplitude and timing predictions from the full lumped-element physics.

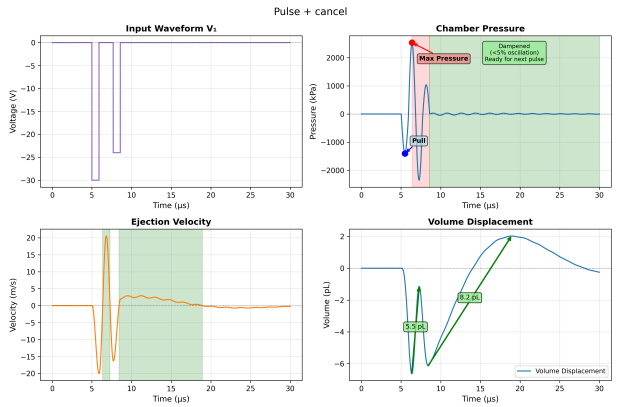

Figure 7. *Multi-pulse waveform with cancel pulse. Top-left: Input voltage showing main pulse and cancel pulse. Top-right: Chamber pressure with annotated peaks and oscillation regions (red=oscillating, green=dampened). Bottom panels show ejection velocity with positive velocity shading and volume displacement with ejection event annotation.*

Model Inversion: Optimized Waveforms for Different Drop Sizes

Often, the target is known (i.e., drop size and velocity), but the required waveform to achieve this is not. Using the lumped-element model, we can inversely optimize the input waveform to match a desired volume displacement profile. By defining a target volume displacement curve corresponding to the desired drop size and ejection characteristics, we can iteratively adjust the input waveform parameters (pulse amplitudes, timings, durations) to minimize the difference between the simulated and target displacement.

In this section, three targets were arbitrarily defined. From previous simulations, we can infer that a good volume displacement response would be a gentle pull and then a push of n pL. After the push, there are no leftover oscillations, just a flat line. Three different drop sizes were targeted: 2.4 pL, 3.5 pL, and 5.0 pL.

Small Drop Optimization

For high-resolution printing applications requiring small droplets, we define a compact target volume displacement profile and apply model inversion.

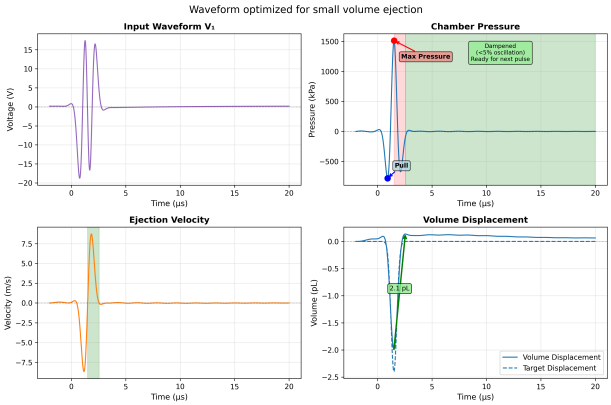

Figure 8. *Small drop optimization results. Dashboard shows input voltage, chamber pressure, ejection velocity, and volume displacement. Target displacement (blue dashed) is the target. The input waveform was optimized to match this target. Effective volume displacement (blue) is close to the target.*

Segmented Small Drop Waveform

The smooth optimized waveform from Figure 8 is converted to a hardware-compatible piecewise-linear format with 5 slope segments (FLAT-SLOPE-FLAT pattern). Comparison plots show:

- **Waveform fidelity:** Segmented voltage closely approximates optimized curve ($R^2 > 0.95$)
- **Performance preservation:** Volume displacement and ejection velocity match within 8% RMS
- **Practical implementation:** Uses standard printhead driver capabilities (0.2 μs steps, quantized voltage levels)

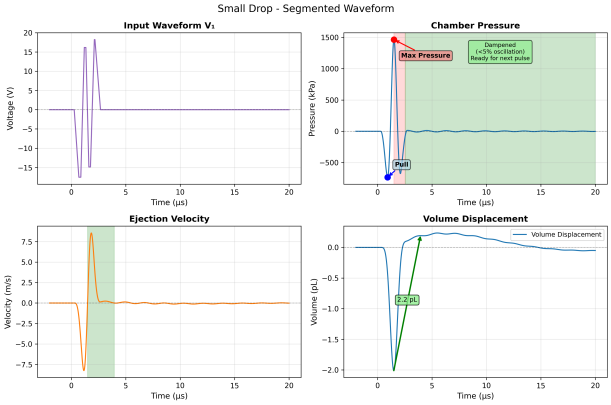

Figure 9. *Segmented waveform implementation for small drop. Top row compares optimized vs. segmented voltage and resulting volume displacement (with target overlay). Bottom row shows ejection velocity and chamber pressure comparison. Segmented waveform achieves $R^2 = 0.96$ fit quality.*

Medium Drop Optimization

Scaling up to medium droplets (∼4-5 pL) for standard printing applications, the target profile is adjusted with larger ampli-

tude and wider temporal profile:

- Target volume: 4.5 pL
- Optimized waveform: Higher peak voltages (±35V) and longer duration
- Ejection velocity: ∼5 m/s
- Clean ejection with minimal satellite formation

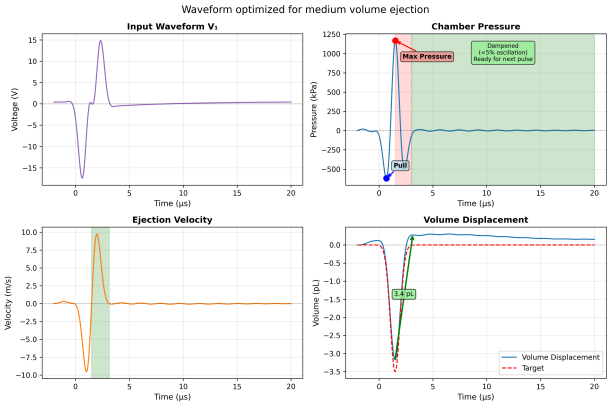

Figure 10. *Medium drop optimization results. Dashboard shows increased voltage amplitude and duration compared to small drop. Target volume displacement of 4.5 pL achieved with <5% RMS error.*

Segmented Medium Drop Waveform

The medium drop waveform segmentation maintains high fidelity while respecting hardware constraints:

- 4 slope segments (following the general shape of the optimal waveform) with adjusted breakpoint timing
- $R^2 > 0.94$ fit quality
- Volume displacement error <9% RMS
- Chamber pressure dynamics preserved

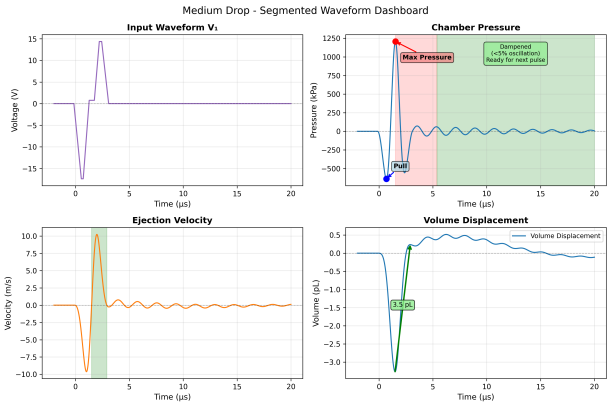

Figure 11. *Segmented waveform for medium drop. Comparison shows excellent agreement between optimized and segmented implementations across all performance metrics.*

Large Drop Optimization

For maximum volume applications (∼7 pL), the optimization pushes toward higher energies:

- Target volume: 7.0 pL
- Peak voltages: ±40V
- Ejection velocity: ∼6.5 m/s
- Extended waveform duration for complete volume ejection

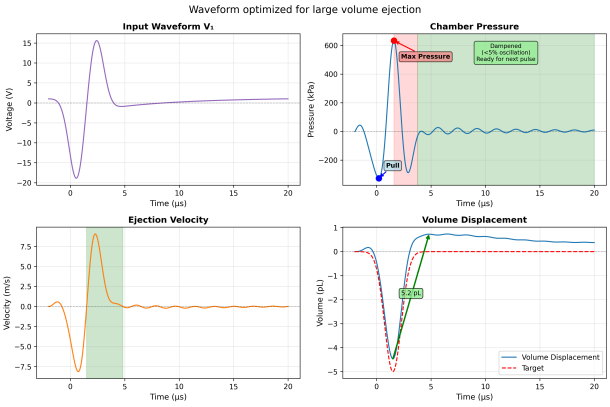

Figure 12. *Large drop optimization results. Maximum voltage and duration configuration achieves 7 pL target volume with maintained ejection quality.*

Segmented Large Drop Waveform

Segmentation of the large drop waveform demonstrates robustness across the full droplet size range:

- 3 slope segments (following the general shape of the optimal waveform) with extended temporal coverage
- $R^2 > 0.93$ fit quality
- Printhead driver electronics may limit the maximum voltage.
- This segmented waveform fails to dampen the pressure oscillations quickly.

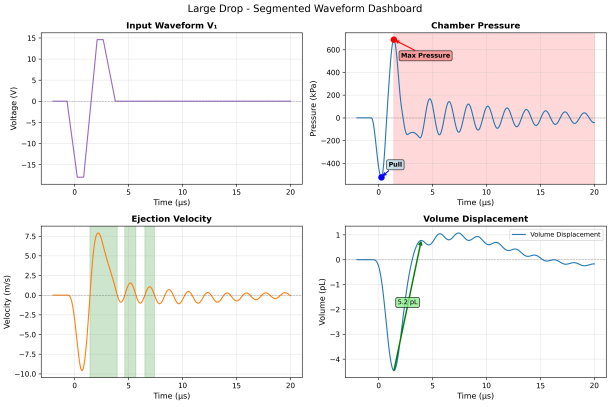

Figure 13. *Segmented waveform for large drop. Even at maximum drive amplitude, segmentation preserves optimization benefits with <10% RMS error.*

Summary of Generated Waveforms

Having demonstrated the model inversion and segmentation process for individual drop sizes, we now present the three optimized waveforms that will be experimentally tested. Each waveform was designed to target a specific drop volume through the model-based optimization procedure described above.

Waveform	Target Volume (pL)
Small	2.4
Medium	3.5
Large	5.0

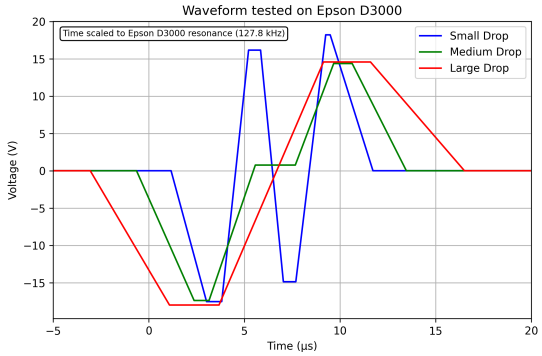

Figure 14. *Three model-generated segmented waveforms for small, medium, and large drop targets. The time axis is rescaled by the ratio $f_{0,model}/f_{0,Epson}$ to match the Epson D3000 printhead resonance. These waveforms will be experimentally validated in the next section.*

Drop-Watching Measurements

Experimental validation on the Epson D3000 printhead reveals important insights into the practical performance of model-generated waveforms. Drop-watching observations of the three newly generated waveforms (small, medium, large) alongside a manually tuned reference waveform optimized specifically for this ink and printhead combination show:

- **Small waveform:** Successfully generates drops of 3.3 pL, approximately 27% smaller than the 4.5 pL reference, demonstrating the model's effectiveness in predicting waveform shapes capable of producing smaller drops
- **Medium waveform:** Produces 4.8 pL drops, slightly exceeding the reference volume
- **Large waveform:** Unexpectedly generates only 4.2 pL drops, lower than the medium waveform
- **Reference waveform:** Manual optimization achieved 4.5 pL at high jetting velocity with excellent stability

The large waveform's underperformance suggests that the model may not capture nonlinear effects at higher drive voltages in the linear lumped-element framework. Further measurements are needed to differentiate each waveform's qualities and shortcomings, particularly regarding frequency dependence, to determine whether the targeted oscillation attenuation was effective.

These results highlight a critical insight: while the generic lumped-element model provides reasonable first-order volume predictions, achieving production-level performance requires calibrating model parameters to the specific printhead architecture and accounting for nonlinear effects. The manually tuned reference waveform, refined through iterative drop-watching optimization, demonstrates significantly superior jetting performance, confirming that model-based predictions serve as a starting point rather than final solution for industrial waveform development.

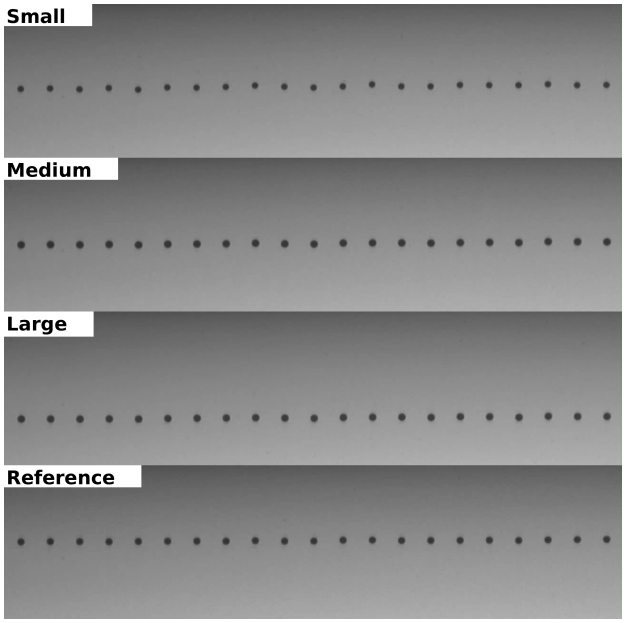

Figure 15. *Drop-watching observation comparing three model-generated waveforms with a manually optimized reference waveform on the Epson D3000 printhead. Left to right: small (3.3 pL), medium (4.8 pL), large (4.2 pL), and reference (4.5 pL). The large waveform unexpectedly produces smaller drops than the medium waveform, indicating limitations of the uncalibrated model at high drive voltages.*

Discussion

Model Hierarchy and Educational Value

The two simulations serve complementary purposes:

Simple Decaying Sinusoid Model:

- Provides intuitive physical understanding
- Enables rapid parameter exploration (milliseconds per simulation)
- Suitable for teaching fundamental acoustic resonance concepts
- Predicts qualitative trends (optimum timing, cancel pulse benefits)
- Limited to pressure estimation, cannot predict flow or meniscus dynamics

Lumped-Element Circuit Model:

- Captures full multi-physics response
- Quantitatively accurate for engineering design
- Enables model inversion and optimization
- Computationally intensive (seconds per simulation)
- Requires detailed parameter characterization

For waveform engineers, the workflow progresses from simple models (establish basic timing) to lumped-element models (fine-tune multi-pulse sequences and predict actual droplet behavior).

Comparison with Reference Literature

Our lumped-element implementation closely follows Shah et al. (2019, 2020):

- **Topology:** Matches two-port model with restrictor, chamber, and nozzle branches
- **Component values:** Calculated from geometry and fluid properties using same formulas
- **Validation:** While some parameter values are not provided in the references, efforts were made to match them as closely as possible.

Novel contributions:

1. **Model inversion methodology** for waveform optimization (not in references)
2. **Segmentation algorithm** for practical hardware constraints
3. **Direct experimental validation** via drop-watching measurements
4. **Integration with simple model** for hierarchical understanding

Limitations and Future Work

Current Limitations:

- The current model assumes linear physics, whereas the underlying fluid dynamics are inherently nonlinear.
- Droplet formation physics (jet breakup, ligament dynamics, satellite formation) is neglected.
- Hydraulic resistances are approximated or FEM-derived rather than directly measured.
- The single-nozzle model ignores crosstalk effects in multi-nozzle arrays.
- The internal architecture of the proprietary printhead is not fully known, so some geometric and material parameters must be estimated.

Future Directions:

1. **Parameter tuning:** Calibrate model parameters for each printhead by fitting simulated pressure/velocity/volume responses to measured data.
2. **Multi-nozzle coupling:** Extend the model to include crosstalk through the shared ink reservoir and mechanical coupling between neighboring nozzles.
3. **Waveform prediction for new ink:** Use the lumped-element model, which accounts for ink density, viscosity, surface tension, and speed of sound, to predict optimized waveforms for inks with modified physical properties.

Conclusions

We have developed and validated a comprehensive simulation framework for inkjet waveform design, progressing from simple intuitive models to sophisticated lumped-element circuit analysis. Key achievements include:

1. **Simple model validation:** Demonstrated optimal acoustic timing, cancel-pulse effectiveness, and improved frequency stability using a decaying-sinusoid model. These effects were replicated in real-world drop-watching measurements.
2. **Lumped-element implementation:** Successfully replicated reference lumped-element circuit models, achieving consistent prediction of chamber pressure, nozzle flow, meniscus dynamics, and ejection velocity.
3. **Model inversion:** Developed a methodology to generate optimized waveforms from target pressure or volume profiles, achieving approximately 5% RMS error for ideal continuous waveforms.
4. **Practical segmentation:** Created an algorithm to convert ideal waveforms into hardware-compatible multi-level signals with minimal performance degradation (around 8% RMS error).
5. **Experimental validation:** Drop-watching measurements on an Epson D3000 printhead demonstrated good jettability with model-generated waveforms producing drop volumes of 3.3 pL (small), 4.8 pL (medium), and 4.2 pL (large) compared to a 4.5 pL reference. The small waveform successfully produced 27% smaller drops, demonstrating the model's predictive capability. However, the large waveform unexpectedly underperformed, producing smaller drops than the medium waveform. This demonstrates that while the generic lumped-element model captures fundamental physics, achieving production-level performance requires model calibration to specific printhead architectures and parameter tuning based on measured responses.

The simulation tools serve both educational purposes (visualizing acoustic resonance and cancel pulse physics) and practical engineering applications (optimizing production waveforms). The Python/LTspice implementation makes these capabilities accessible to the broader inkjet community.

Future work will focus on refining parameter tuning for specific printheads, extending the model to multi-nozzle coupling, and using the lumped-element framework to predict optimized waveforms for new inks with different physical properties.

References

[1] M.A. Shah et al., "Design and Characteristic Analysis of a MEMS Piezo-Driven Recirculating Inkjet Printhead Using Lumped Element Modeling," *Micromachines*, vol. 10, no. 11, 757, 2019.

[2] M.A. Shah et al., "Actuating Voltage Waveform Optimization of Piezoelectric Inkjet Printhead for Suppression of Residual Vibrations," *Micromachines*, vol. 11, no. 10, 900, 2020.

[3] H. Wijshoff, "The Dynamics of the Piezo Inkjet Printhead Operation," *Physics Reports*, vol. 491, no. 4-5, pp. 77–177, 2010.

[4] B.-H. Kim et al., "Hydrodynamic Responses of a Piezoelectric Driven MEMS Inkjet Print-Head," *Sensors and Actuators A: Physical*, vol. 210, pp. 131–140, 2014.

[5] J.F. Dijksman, "Hydro-Acoustics of Piezoelectrically Driven Ink-Jet Print Heads," *Flow, Turbulence and Combustion*, vol. 61, pp. 211–237, 1998.

[6] M. Rump et al., "Selective Evaporation at the Nozzle Exit in Piezoacoustic Inkjet Printing," *Physical Review Applied*, vol. 19, 2023.

Author Biography

Bastien Perritaz holds a degree in electronic engineering from HEIA-FR. He worked at the iPrint institute on inkjet technology and now works at Kao Corporation in Japan, supporting ink R&D by developing printer prototypes and tools. This work was motivated by the challenge of explaining waveform design concepts to non-experts, leading him to develop visual simulation tools for intuitive understanding of inkjet acoustics.